JOURNAL OF PHYSICAL ORGANIC CHEMISTRY
J. Phys. Org. Chem. 2002; **15:** 742–749
Published online in Wiley InterScience (www.interscience.wiley.com). DOI: 10.1002/poc.545

Molecular polarizability of fullerenes and endohedral metallofullerenes

Francisco Torrens*

Institut Universitari de Ciència Molecular, Universitat de València, Dr. Moliner 50, E-46100 Burjassot (València), Spain

Received 31 January 2002; revised 10 May 2002; accepted 7 June 2002

ABSTRACT: The interacting induced dipoles polarization model implemented in our program POLAR is used for the calculation of the molecular dipole $\overline{\mu}$ and tensor quadrupole $\overline{\overline{\Theta}}$ moments and also the dipole–dipole polarizability $\overline{\overline{\alpha}}$.The method is tested with Sc_n, C_n (fullerene and graphite) and endohedral $Sc_n@C_m$ clusters. The polarizability is an important quantity for the identification of clusters with different numbers of atoms and even for the separation of isomers. The results for the polarizability are of the same order of magnitude as from reference calculations performed with our version of the program PAPID. The bulk limit for the polarizability is estimated from the Clausius–Mossotti relationship. The polarizability trend for these clusters as a function of size is different from what one might have expected. The clusters are more polarizable than what one might have inferred from the bulk polarizability. Previous theoretical work yielded the same trend for Si_n, Ge_n and Ga_nAs_m small clusters. However, previous experimental work yielded the opposite trend for Si_n, Ga_nAs_m and Ge_nTe_m larger clusters. At present, the origin of this difference is problematic. One might argue that smaller clusters need not behave like those of intermediate size. The high polarizability of small clusters is attributed to dangling bonds at the surface of the cluster. In this respect, semiconductor clusters resemble *metallic* clusters. Copyright © 2002 John Wiley & Sons, Ltd.

KEYWORDS: dipole moment; quadrupole moment; polarization; polarizability; nanostructure; scandium cluster; fullerene; graphite

INTRODUCTION

Benichou *et al.* measured the static electric dipole polarizabilities of Li_n ($2 \leq n \leq 22$) clusters.[1] Maroulis and Xenides reported highly accurate *ab initio* calculations for Li_4.[2] An extensive investigation of basis set and electron correlation effects led to dipole polarizability values of $\overline{\alpha} = 387.01$ a.u. Their values for the mean polarizability were systematically higher than the recently reported experimental value (326.6 a.u.).

Fuentealba calculated the polarizability of C_n ($n \leq 8$) clusters using density functional theory (DFT) with hybrid-type functionals in combination with the finite-field method.[3] In particular, he predicted that the jet formed by both isomers of C_6, cyclic and linear, would split up in the presence of an electric field. Fuentealba and Reyes calculated the polarizability of a series of Li_nH_m clusters using DFT.[4]

Jackson *et al.* used DFT to calculate the polarizabilities for several low-energy geometries of Si_n ($10 \leq n \leq 20$) clusters.[5] The calculations indicated that the polarizability per atom for Si clusters approaches the bulk limit from above as a function of size. Deng and co-workers calculated the polarizabilities of Si_n ($9 \leq n \leq 28$) clusters using DFT.[6,7] They used geometrics carefully selected by energy minimization. The polarizability showed fairly irregular variations with cluster size, but all calculated values were higher than the bulk value.

Hohm *et al.* deduced an experimental value of 116.7 ± 1.1 a.u. for the polarizability of As_4 from the analysis of refractivity measurements in arsenic vapour.[8] This was in close agreement with the *ab initio* finite-field many-body perturbation theory and coupled-cluster calculation result of 119.5 ± 3.6 a.u.

The present author has tried to develop a scheme (POLAR) that is less demanding in time and resources than are first-principle calculations such as DFT and PAPID. The final aim of POLAR will be its application to large molecules and assemblies. A further use of POLAR will be to differentiate those atoms with the same atomic number in a molecule (e.g. central and ending O atoms in O_3). The price to be paid in both PAPID and POLAR is then the necessity for semiempirical calibrations. However, POLAR does not require a particular calibration for each new molecule. In this work, POLAR was applied to the following clusters: Sc_1–Sc_7, Sc_{12}, Sc_{17}–HCP and Sc_{74}–HCP, C, C_{12}, C_{60}, C_{70} and C_{82} (fulllerene), $Sc@C_{60}$, $Sc@C_{82}$, $Sc_2@C_{82}$ and $Sc_3@C_{82}$ (endohedral), and C_1–C_6, C_{10}, C_{13}, C_{16}, C_{19}, C_{22}, C_{24}, C_{42}, C_{54}, C_{84} and C_{96} (graphite).

**Correspondence to:* F. Torrens, Institut Universitari de Ciència Molecular, Universitat de València, Dr. Moliner 50, E-46100 Burjassot (València), Spain.
E-mail: francisco.torrens@uv.es
Contract/grant sponsor: Spanish MCT (Plan Nacional I+D+I); *Contract/grant number:* BQU2001-2935-C02-01.

In the next section, the interacting induced dipoles polarization model for molecular polarizabilities is presented. Next, the improvements in the polarization model are introduced. A description of the programs PAPID and POLAR is given in the two following sections. Following that, results are presented and discussed. The last section summarizes the conclusions.

INTERACTING INDUCED DIPOLES POLARIZATION MODEL FOR MOLECULAR POLARIZABILITIES

The calculation of molecular polarizabilities has been carried out by the interacting induced dipoles polarization model,[9–11] which calculates tensor effective anisotropic point polarizabilities[12–14] by the method of Applequist *et al.*[15,16] One considers the molecule as being made up of N atoms (represented by $i, j, k, \ldots$), each of which acts as a point particle located at the nucleus and responds to an electric field only by the induction of a dipole moment, which is a linear function of the local field. If a Cartesian component of the field due to the permanent multipole moments is E_a^i, then the induced moment μ_a^i in atom i is

$$\mu_a^i = \alpha^i \left[E_a^i + \sum_{j(\neq i)}^{N} T_{ab}^{ij} \mu_b^j \right] \tag{1}$$

where α^i is the polarizability of atom i and T_{ab}^{ij} is the symmetrical field gradient tensor, $T_{ab}^{ij} = 1/e\nabla_a^i E_b^j$, where e is the charge of the proton and the subscripts *a, b, c, …* stand for the Cartesian components *x, y, z*. In Eqn. (1), the expression in brackets is the total electric field at atom i, consisting of the external field plus the fields of all the other induced dipoles in the molecule.

The set of coupled linear Eqns (1) for the induced dipole moments can be expressed conveniently in compact matrix equation form, if one introduces the $3N \times 3N$ matrices $\overline{\overline{T}}$ and $\overline{\overline{\alpha}}$, with elements T_{ab}^{ij} and $\alpha_{ab}^i \delta^{ij}$ (δ^{ij} being the Kronecker δ), respectively. To suppress the restriction in the sum, the diagonal elements T_{ab}^{ij} are defined as zero. Similarly, $\overline{E}$ and $\overline{\mu}$ are $3N \times 1$ column vectors with elements E_a^i and μ_a^i. Equation (1) is thus written in matrix form as

$$\overline{\mu} = \overline{\overline{\alpha}}\left(\overline{\overline{I}}\,\overline{E} + \overline{\overline{T}}\,\overline{\mu}\right) = \overline{\overline{\alpha}}\,\overline{\overline{I}}\,\overline{E} + \overline{\overline{\alpha}}\,\overline{\overline{T}}\,\overline{\mu}$$

where $\overline{\overline{I}}$ is the $3N \times 3N$-dimensional unit matrix. This matrix equation can be solved for the induced dipoles as

$$\overline{\mu} = \left(\overline{\overline{I}} - \overline{\overline{\alpha}}\,\overline{\overline{T}}\right)^{-1} \overline{\overline{\alpha}}\,\overline{E} = \overline{\overline{A}}\,\overline{E}$$

Here the symmetrical many-body polarizability matrix $\overline{\overline{A}}$ has been introduced:

$$\overline{\overline{A}} = \left(\overline{\overline{I}} - \overline{\overline{\alpha}}\,\overline{\overline{T}}\right)^{-1} \overline{\overline{\alpha}}$$

The compact matrix equation $\overline{\mu} = \overline{\overline{A}}\,\overline{E}$ is equivalent to the N matrix equations:

$$\overline{\mu}^i = \sum_{j=1}^{N} \overline{\overline{A}}^{ij}\,\overline{E}^j$$

Let the molecule be in a uniform applied field, so that $\overline{E}^j = \overline{E}$ for all j. Then this equation becomes

$$\overline{\mu}^i = \left[\sum_{j=1}^{N} \overline{\overline{A}}^{ij}\right] \overline{E} = \overline{\overline{\alpha}}^{\,eff,i}\,\overline{E}$$

The coefficient of $\overline{E}$ in this equation is seen to be an effective polarizability of unit i, $\overline{\alpha}^{eff,i}$.The total moment induced in the molecule $\overline{\mu}^{mol}$ is

$$\overline{\mu}^{mol} = \sum_{i=1}^{N} \overline{\mu}^i = \left[\sum_{i=1}^{N}\sum_{j=1}^{N} \overline{\overline{A}}^{ij}\right] \overline{E} = \left[\sum_{i=1}^{N} \overline{\overline{\alpha}}^{\,eff,i}\right] \overline{E}$$

from which it is seen that the molecular polarizability tensor $\overline{\overline{\alpha}}^{mol}$ is

$$\overline{\overline{\alpha}}^{\,mol} = \sum_{i=1}^{N}\sum_{j=1}^{N} \overline{\overline{A}}^{ij} = \sum_{i=1}^{N} \overline{\overline{\alpha}}^{\,eff,i}$$

IMPROVEMENTS IN THE POLARIZATION MODEL

The following improvements have been implemented in the model:

1. A damping function has been used in the calculation of the symmetrical field gradient tensor in order to prevent the polarizability from going to infinity.[17]
2. The interaction between bonded atoms and atoms with a distance lying in an interval defined by $[r^{\inf}, r^{\sup}]$ has been neglected. The starting values for this interval are $[0,10^{30}]$ and $r^{\inf}$ is incremented if resonance conditions are detected.
3. To build up the many-body polarizability matrix $\overline{\overline{A}}$, the atomic polarizability tensors given by $\overline{\overline{\alpha}}^{\,i} = \overline{\overline{\alpha}}_{\sigma}^{\,i} + \overline{\overline{\alpha}}_{\pi}^{\,i}$ have been used instead of the scalar polarizability α^i.

DESCRIPTION OF PROGRAM PAPID

PAPID carries out the calculation of molecular electric polarizabilities using an isotropic atom point dipole model without interaction, an isotropic atom point dipole

interaction model or an anisotropic atom point dipole interaction model.[18] PAPID allows the following polarization options: (1) model of atomic dipoles μ^i without interaction; (2) model of μ^i with optimization of isotropic atomic polarizabilities α^i; (3) iterative Applequist model (μ^i interacting with isotropic α^i); (4) iterative Applequist model with optimization of α^i; (5) non-iterative Applequist model; (6) non-iterative Applequist model with optimization of α^i; (7) iterative Birge model (μ^i interacting with anisotropic α^i);[19] (8) iterative Birge model with optimization of α^i; (9) iterative Birge model with optimization of α^i and atomic anisotropy constants ζ^i; (10) iterative Birge model with optimization of α^i and one-centre valence state electron repulsion integrals g^i; (11) non-iterative Birge model; (12) non-iterative Birge model with optimization of α^i; (13) non-iterative Birge model with optimization of α^i and ζ^i; and (14) non-iterative Birge model with optimization of α^i and g^i.

The optimization of the atomic parameters allows selection between the Fletcher method[20] and the Lagrange three-point extrapolation. The Fletcher algorithm allows selection of the precision on the stability of the minimum obtained from the optimization of the atomic parameters among a vast extrapolation of surfaces associated with a weak stability of the minima, an intermediate value and a good stability of the obtained minimum associated with a weak modification of the parameters at each iteration of the optimization process. PAPID allows a choice of whether to use vibrational corrections obtained by a modification of the increments for the atomic polarizabilities. The input of Cartesian coordinates allows selection between atomic units and ångstroms. The input allows the choice of whether to include the dipole–quadrupole polarizability matrix $\overline{\overline{A}}$.The optimization of the atomic parameters allows selection between the fitting of the molecular dipole–dipole polarizabilities α_{ab} and the simultaneous fitting of α_{ab} and all the non-zero components $A_{a,bc}$ of matrix $\overline{\overline{A}}$.

The inversion of the many-body polarizability matrix $\overline{\overline{A}}$ allows selection between the analytical (iterative) and perturbative (non-iterative) methods. The analytical calculation allows selection of the test level on the obtained results among no test, test on the stability of the determinant of matrix $\overline{\overline{A}}$ and test on the stability of the determinant and eigenvalues of matrix $\overline{\overline{A}}$.The perturbative treatment calculates up to the fourth-order perturbation. The analytical expression of the dyadic operator for dipolar interaction allows the choice of whether to use the Thole method for the modification of the analytical form for the dyadic tensors as a function of the value for the relative position R_{ij} of atoms i and j.[21] PAPID allows a choice of whether to take into account the dipolar interactions between bonded atoms. Moreover, the dipolar interaction between atoms i and j can be cut off by an upper radius describing the outer limit of the interaction sphere, centred on unit i. Furthermore, their dipolar interaction can be cut off by the radius of a sphere centred on i and containing no interaction.

PAPID contains a database of optimized polarization parameters for the following atomic classes: H [alkane, alcohol, aldehyde, amide, amine and amine ion$^{(+)}$], C [alkane, carbonyl, alcohol, amine, amide, carboxylic acid/ester and carboxylate$^{(-)}$], N [amide, amine and amine ion$^{(+)}$], O [alcohol, ether, carbonyl, carboxylic acid/ester and carboxylate$^{(-)}$], F (halomethanes), Cl (halomethanes), Br (halomethanes) and I (halomethanes).

The following improvements have been implemented in our version of PAPID:

1. The calculation can start from a predefined value of $r^{\inf}$ and increment $r^{\inf}$ by one atomic unit, each time resonance conditions are detected, up to $r^{\sup}$.
2. The atomic polarizabilities allow selection between optimized *ab initio* and experimental values.
3. The atomic classes can be either read from input or assigned by the program.
4. The molecule can be reoriented by its principal axes of inertia.
5. The polarization parameters have been included in the database for He, Li, Be, B, Ne, Na, Mg, Al, Si, P, S, Ar, K, Ca, Sc, Ti, V, Cr, Mn, Fe, Co, Ni, Cu, Zn, Ga, Ge, As, Se, Kr, Rb, Sr, Y, Zr, Nb, Mo, Tc, Ru, Rh, Pd, Ag, Cd, In, Sn, Sb, Te and Xe.
6. The optimized experimental polarization parameters have been included in the database for the following atomic classes: H (alkane, alcohol, aldehyde, amide, amine and aromatic), C (alkane, carbonyl, nitrile and aromatic), N (amide, amine and nitrile), O (alcohol, ether and carbonyl), F (halomethanes), Cl (halomethanes), Br (halomethanes) and I (halomethanes).[22]

DESCRIPTION OF PROGRAM POLAR

POLAR carries out the calculation of molecular electric polarizablities and allows selection between the iterative Applequist model (isotropic α^i) and the iterative Birge model (anisotropic α^i).[23] POLAR allows a choice of whether to re-orientate the molecule by its principal axes of inertia. In describing the partial charge method developed for the Mulliken scale,[24] Huheey mentioned that most elements approximately double their electronegativities as the partial charge approaches $+1$ whereas their electronegativities essentially disappear as the partial charge approaches -1.[25] The Mulliken and Pauling scales are roughly proportional, so Huheey's observation may be expressed in Pauling units as

$$X_{eq} = X_A + \Delta_A X_A$$

where, X_{eq} is the electronegativity as equalized through Sanderson's principle, X_A is the initial, pre-bonded

electronegativity of a particular atom A and Δ_A is the σ partial charge on A.[26] Charge conservation leads to a general expression for X_{eq}:

$$X_{eq} = \frac{N + q}{\sum\limits_{atoms} \frac{v_A}{X_A}}$$

where $N = \sum v$ equals the total number of atoms in the species formula and q is the σ molecular charge. The σ partial charge Δ_A on atom A can be generalized as

$$\Delta_A = \sum_{bonds} \frac{X_{eq,b} - X_A}{X_A}$$

and the electronegativity equalized for bonds is given as

$$X_{eq,b} = \frac{2 + \frac{q}{m}}{\frac{1}{X_A} + \frac{1}{X_B}}$$

where m is the number of bonds in the molecule.

The π-net charges and polarizabilities have been evaluated with the Hückel molecular orbital (HMO) method. It is well known that π-conjugation vanishes for perpendicular structures (e.g. biphenyl). The HMO β parameter can be evaluated, to a first approximation, between p_z orbitals twisted from coplanarity by an angle θ as

$$\beta = \beta_0 \cos\theta$$

where β_0 is equal to the β parameter for benzene.[27] Joachim *et al.* evaluated the electronic coupling V_{ab} of the binuclear mixed-valence M^{II}–L–M^{III} complex $[(NH_3)_5Ru$–bipyridyl–$Ru(NH_3)_5]^{5+}$.[28] When a pyridine ring rotates around the ligand axis, $\pi - \pi$ $V_{ab}(\theta)$ can be best fitted by a $\cos^{1.15}\theta$ function. From this observation, the β function is assumed universal and has the same form as V_{ab} for this complex:

$$\beta = \beta_0 \cos^{1.15}\theta$$

The dipole and tensor quadrupole moments have been calculated from the point distribution of net charges. The dipole moment vector is calculated as

$$\mu_a = \sum_i q^i r_a^i$$

and the quadrupole moment tensor is calculated as

$$\theta_{ab} = \theta_{ba} = \frac{1}{2}\sum_i q^i \left[3 r_a^i r_b^i - \left(r^i\right)^2 \delta_{ab}\right]$$

where q^i is the ith element of charge at the point $\bar{r}^i$ relative to an origin fixed at the centre of mass in the molecule. δ_{ab} is the Kronecker δ. The subscripts *a, b, …* denote vector or tensor components and can be equal to the Cartesian components *x, y, z*. Only the first, non-vanishing moment is independent of the choice of origin. Thus for an ion such as OH^-, the dipole and quadrupole moments vary with the origin, and $\mu = 0$ at the *centre of charge*. Similarly, in HF, Θ depends on origin and is zero at the *centre of dipole*. In order to avoid these dependences, the molecule is brought into its principal internal coordinate system, e.g. linear molecules on the *x*-axis and planar molecules on the *xy* plane.

It can be shown that for every square matrix $\overline{\overline{\Theta}}$ there exists a matrix $\overline{\overline{V}}$ and its inverse $\overline{\overline{V}}^{-1}$, which transforms $\overline{\overline{\Theta}}$ to a diagonal matrix $\overline{\overline{D}}$.[29]

$$\overline{\overline{D}} = \overline{\overline{V}}^{-1}\,\overline{\overline{\Theta}}\,\overline{\overline{V}} = \mathrm{diag}(\Theta_1, \Theta_2, \Theta_3)$$

where scalar Θ_i are the eigenvalues of matrix $\overline{\overline{\Theta}}$. The right eigenvectors of $\overline{\overline{\Theta}}$ are non-zero column vectors $\bar{x}$ such that satisfy the following equation:

$$\overline{\overline{\Theta}}\bar{x} = \Theta_i \bar{x}$$

The eigenvectors are independent of the choice of origin and are easily compared with other values. Moreover, the reduction from nine Θ_{ab} matrix elements in $\overline{\overline{\Theta}}$ (actually six because $\overline{\overline{\Theta}}$ is symmetric) to three facilitates the comparison with another results.

The trace of a square matrix $\overline{\overline{\Theta}}$ is defined as the sum of its diagonal elements:

$$\mathrm{Tr}\left(\overline{\overline{\Theta}}\right) = \Theta_{xx} + \Theta_{yy} + \Theta_{zz} = \Theta_1 + \Theta_2 + \Theta_3$$

The trace is independent of the choice of origin and can be calculated in Cartesian coordinates or from the eigenvalues. The mean of a 3×3 square matrix $\overline{\overline{\Theta}}$ is defined as

$$\Theta = \frac{\mathrm{Tr}\left(\overline{\overline{\Theta}}\right)}{3} = \frac{\Theta_{xx} + \Theta_{yy} + \Theta_{zz}}{3} = \frac{\Theta_1 + \Theta_2 + \Theta_3}{3}$$

The starting atomic polarizabilities are evaluated from the atomic net charges. Sanderson's principle allows the calculation of the σ atomic polarizabilities as

$$\alpha_A = \frac{\partial \Delta_A}{\partial X_A} = \sum_{bonds} \frac{f_A s_A (1 - \Delta_A)\left(2 - \frac{q}{m}\right) X_B}{(2 - \Delta_A - \Delta_B)(X_A + X_B)^2}$$

where the coefficients f_A and s_A have been introduced to take into account the effects of the atomic charge (Δ_A), internal sub-shells and lone pairs on α_A. f_A is calculated as

$$f_A = 1 - 1.5\Delta_A + 0.5\Delta_A^2$$

and s_A is calculated as

$$s_A = C_A + 0.15 L_A$$

where C_A is related to the number of internal sub-shells [C_A = 1 (H–Ne), 3 (Na–Ar), 4 (K–Zn), 5 (Ga–Kr), 6 (Rb–Cd) and 7 (In–Xe)] and L_A is the number of lone pairs on atom A. The σ tensor atomic polarizabilities are calculated according to

$$\overline{\overline{\alpha}}_\sigma = \sum_{bonds} \frac{3\alpha_\sigma}{\alpha^{\parallel} + 2\alpha^{\perp}} \begin{bmatrix} \alpha^{\perp} & 0 & 0 \\ 0 & \alpha^{\perp} & 0 \\ 0 & 0 & \alpha^{\parallel} \end{bmatrix} = \sum_{bonds} \frac{3\alpha_\sigma}{3.676} \begin{bmatrix} 1 & 0 & 0 \\ 0 & 1 & 0 \\ 0 & 0 & 1.676 \end{bmatrix}$$

where the z-axis is defined as the bond direction for each bond. The diagonal form of $\overline{\overline{\alpha}}_\sigma$ has two distinct components denoted $\alpha^{\parallel}$ and $\alpha^{\perp}$, parallel and perpendicular, respectively, to the bond axis. The parameter $\alpha^{\parallel}/\alpha^{\perp} = 1.676$ has been obtained by fitting the isotropic bonding polarizabilities of Vogel.[30] The bonding polarizabilities have been implemented in the database of program SIBFA.[31].

The π tensor atomic polarizabilities are calculated as

$$\overline{\overline{\alpha}}_\pi = \sum_{bonds} \frac{3\alpha_\pi}{2\alpha^{\parallel} + \alpha^{\perp}} \begin{bmatrix} \alpha^{\parallel} & 0 & 0 \\ 0 & \alpha^{\parallel} & 0 \\ 0 & 0 & \alpha^{\perp} \end{bmatrix} = \sum_{bonds} \frac{3\alpha_\pi}{3.741} \begin{bmatrix} 1 & 0 & 0 \\ 0 & 1 & 0 \\ 0 & 0 & 1.741 \end{bmatrix}$$

where the xy plane is the σ-plane. $\alpha^{\parallel}$ and $\alpha^{\perp}$ are parallel and perpendicular, respectively, to the σ-plane. The parameter $\alpha^{\perp}/\alpha^{\parallel} = 1.741$ has been obtained by fitting the experimental polarizabilities of aromatic molecules.

POLAR allows the choice of whether to take into account the dipolar interactions between bonded atoms. Moreover, the dipolar interaction between a pair of atoms can be cut off by lower and upper radii describing the inner and outer limits of the interaction sphere.

A fully operative version of POLAR, including the whole interacting induced dipoles polarization model, has been implemented in the molecular mechanics program MM2[32] and in the empirical conformational energy program for peptides ECEPP2.[33] The new versions are called MMID and ECEPPID, respectively.

CALCULATION RESULTS AND DISCUSSION

In this work, the geometries of the clusters were optimized with our program MMID. The dipole $\overline{\mu}$ and tensor quadrupole $\overline{\overline{\Theta}}$ moments of the Sc_n C_n and caged $Sc_n@C_m$ clusters are reported in Table 1. Some clusters are polar whereas others are apolar. Dipole moments are presented for clusters of tetrahedral (T_d), octahedral (O_h) and D_{3d} symmetry. Note that a molecule of T_d symmetry, such as methane, does not have a permanent dipole moment.[34] This is due to the full occupation of the $(\sigma_s)(\sigma_x, \sigma_y, \sigma_z)$ orbitals with eight electrons. However, Sc_4 has a partial occupation of the corresponding orbitals with four electrons. The stereochemical consequence of this configuration is that Sc_4 suffers Jahn–Teller distortion in a tetrahedral environment. As a consequence, a dipole moment can appear. Similar Jahn–Teller effects occur in O_h and $D_{3d}Sc_6$ clusters. On the other hand, some polar and apolar clusters show negative mean Θ. Mean Θ is always either near zero or negative. In particular, for C_{60} and C_{82}, μ and mean Θ remain almost constant after the inclusion of one endohedral Sc atom. However, the inclusion of two or three caged Sc atoms in C_{82} strongly increases both μ and minus mean Θ.

The elementary dipole–dipole polarizabilities $<\alpha>$ for the Sc_n clusters are listed in Table 2. For all the clusters, POLAR somewhat underestimates $<\alpha>$ when compared with the PAPID results. In particular, for Sc_1, POLAR and PAPID results are equally underestimated with respect to the numerical restricted Hartree–Fock (RHF) value calculated by Stiehler and Hinze (22.317 Å^3).[35]

The variation of the computed values for the elementary polarizability with the number of Sc atoms is illustrated in Fig. 1(a). The results for the three Sc_4 isomers are nearly equal and so they are superimposed with POLAR. Similarly, both Sc_6 isomers are superposed with PAPID. On varying the number of atoms, the clusters show numbers indicative of particularly polarizable structures. Despite the PAPID results for the small clusters tend to the bulk limit, both clusters in the HCP structure move from this limit. Hence both HCP cluster results should be treated with care. As a reference, the bulk limit for the polarizability has been calculated from the Clausius–Mossotti relationship:

$$\alpha = \frac{3(\varepsilon - 1)v}{4\pi(\varepsilon + 2)}$$

where v is an elementary volume per atom in the crystalline state and ε is the bulk dielectric constant. For metals, ε approaches infinity and the dependence of α on ε disappears. In this work, for Sc the v value used is 15.0 Å^3 per atom and α is calculated as 3.581 Å^3 per atom, and for C, v = 5.3 Å^3 and α = 1.265 Å^3.

The polarizability trend for the Sc_n clusters as a function of size is different from what one might have expected. The Sc_n clusters calculated with POLAR and PAPID are, in general, more polarizable than what one might have inferred from the bulk. Previous theoretical work with DFT within the one-electron approximation yielded the same trend for Si_n, Ge_n and Ga_nAs_m small clusters. However, previous experimental work yielded

Table 1. Electrostatic properties for the clusters

Cluster	μ (D)[a]	Θ (D Å)[b]	Θ_1[c]	Θ_2	Θ_3
Sc	0.000	0.000	0.000	0.000	0.000
Sc_2	0.000	0.000	0.000	0.000	0.000
Sc_3	8.167	0.000	6.943	0.000	−6.944
$Sc_4 D_{4h}$	0.000	0.000	20.673	0.000	−20.673
$Sc_4 D_{2h}$	0.000	−5.259	7.889	0.000	−23.666
$Sc_4 T_d$[d]	2.310	0.000	2.332	0.140	−2.472
Sc_5	0.000	−3.056	4.584	4.584	−18.338
$Sc_6 O_h$[d]	1.753	−14.560	5.304	−3.316	−13.528
$Sc_6 D_{3d}$[d]	0.220	0.000	6.009	−0.642	−5.367
Sc_7	7.501	−1.687	3.129	−3.486	−4.706
Sc_{12}	5.042	0.000	16.407	−6.665	−9.741
C	0.000	0.000	0.000	0.000	0.000
C_{12}	2.414	0.000	3.761	−1.528	−2.233
C_{60}	0.000	0.000	0.000	0.000	0.000
$Sc@C_{60}$	0.000	0.000	0.000	0.000	0.000
C_{70}	0.000	−0.165	0.954	−0.725	−0.725
C_{82}	8.345	0.063	6.073	3.589	−9.472
$Sc@C_{82}$	8.345	0.061	6.075	3.589	−9.481
$Sc_2@C_{82}$	15.737	−45.889	−33.445	−49.945	−54.278
$Sc_3@C_{82}$	17.736	−43.580	−33.443	−47.334	−49.963

[a] Dipole moment.
[b] Mean quadrupole moment.
[c] Quadrupole moment tensor eigenvalues Θ_1, Θ_2 and Θ_3.
[d] Structures with Jahn–Teller distortion.

the opposite trend for Si_n, Ga_nAs_m and Ge_nTe_m larger clusters.[36] At present, the origin of this difference is problematic. One might argue that smaller clusters need not behave like those of intermediate size. In addition, the error bars in the experiments are fairly large.

The high polarizability of the Sc_n clusters is attributed to dangling bonds at the surface of the cluster. Indeed, most of the atoms within small clusters reside on the surface. In this respect, semiconductor clusters resemble *metallic* clusters. They tend to have higher coordination numbers than those in the crystalline state. In fact, these structures are thought more closely related to the high-pressure metallic phases than to the diamond structure.[37] For example, it has been shown that the polarizabilities of alkaline metal clusters significantly exceed the bulk limit and tend to decrease with increasing cluster size.[38,39]

Table 2. Elementary molecular dipole–dipole polarizabilities for Sc clusters

Sc_n	$<\alpha>$(Å^3)[a]	$<\alpha>_{ref.}$[b]
Sc	16.893	16.893
Sc_2	4.524	13.744
Sc_3	6.885	11.557
Sc_4 D_{4h}	6.613	12.873
Sc_4 D_{2h}	7.170	11.163
Sc_4 T_d	7.288	10.041
Sc_5	7.546	9.690
Sc_6 O_h	8.306	10.330
Sc_6 D_{3d}	9.810	10.330
Sc_7	7.596	9.321
Sc_{12}	8.383	8.724
Sc_{17} h.c.p.	7.819	25.278
Sc_{74} h.c.p.	23.143	23.471

[a] Average dipole–dipole polarizability.
[b] Reference: calculations carried out with the PAPID program.

The elementary polarizability for the fullerenes and one-shell graphite models is collected in Table 3. For all the fullerenes, POLAR rather overestimates $<\alpha>$ when compared with PAPID. In particular, for C_1 the POLAR result lies between the PAPID and the numerical RHF value (1.783 Å^3) of Stiehler and Hinze[35] or the DFT result of Fuentealba (1.882 Å^3).[3] For C_{60}, the POLAR result is closer to the experimental values measured by Ballard *et al.* (1.32 ± 0.07 Å^3)[40] and Antoine *et al.* (1.28 ± 0.13 Å^3)[41] and to the *ab initio* value calculated by Norman *et al.* (1.430 Å^3)[42] than is the PAPID calculation. For C_{70}, the POLAR result is very much closer to the experimental value measured by Compagnon *et al.* (1.5 ± 0.2 Å^3)[43] than is the PAPID evaluation. For all the graphite models, POLAR rather overestimates $<\alpha>$ compared with PAPID. In particular, for C_6-cyclic compounds the POLAR result is closer to the DFT value (1.445 Å^3) of Fuentealba[3] than is the PAPID result.

All the fullerenes calculated with POLAR are more polarizable than the bulk [cf. Fig. 1(b)]. However, the PAPID results for large fullerenes are less polarizable than the bulk. In turn, the one-shell graphite models calculated with POLAR are more polarizable than the bulk [cf. Figure 1(c)]. However, the PAPID results are, in general, less polarizable than the bulk.

The elementary polarizabilities for the endohedral $Sc_n@C_m$ fullerenes are given in Table 4. The elementary

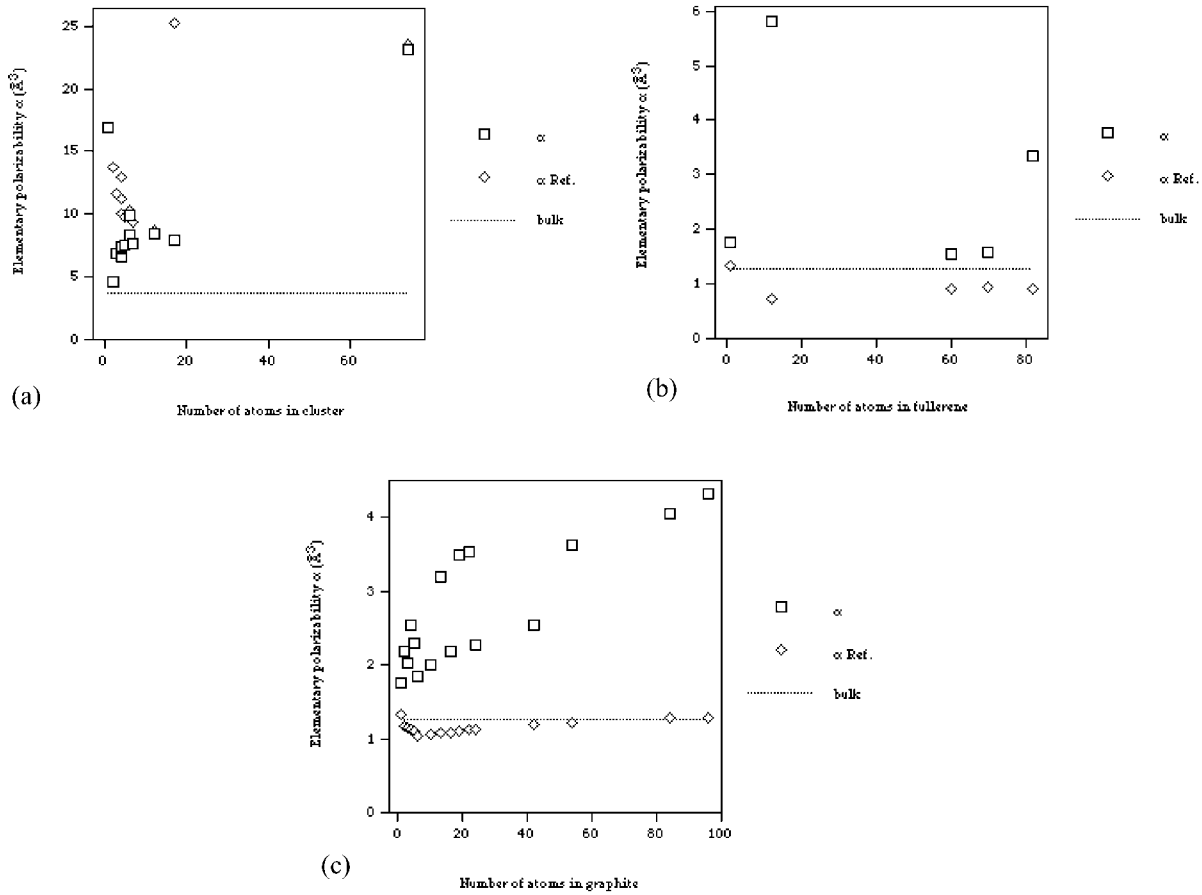

Figure 1. Average atom–atom polarizabilities per atom vs cluster size for (a) Sc_n clusters, (b) fullerenes and (c) one-shell graphite models. Dotted lines correspond to the bulk polarizabilities

Table 3. Elementary molecular dipole–dipole polarizabilities for fullerenes and one-shell graphite models

	Fullerene		Graphite	
C_n	$<\alpha>$(Å^3)[a]	$<\alpha>_{ref.}$[b]	$<\alpha>$[a]	$<\alpha>_{ref.}$[b]
C	1.763	1.322	1.763	1.322
C_2	—	—	2.187	1.160
C_3	—	—	2.017	1.153
C_4	—	—	2.545	1.130
C_5	—	—	2.303	1.097
C_6	—	—	1.834	1.024
C_{10}	—	—	2.009	1.067
C_{12}	5.825	0.722	—	—
C_{13}	—	—	3.186	1.074
C_{16}	—	—	2.180	1.091
C_{19}	—	—	3.491	1.109
C_{22}	—	—	3.539	1.116
C_{24}	—	—	2.280	1.117
C_{42}	—	—	2.538	1.185
C_{54}	—	—	3.633	1.212
C_{60}	1.546	0.904	—	—
C_{70}	1.579	0.920	—	—
C_{82}	3.349	0.911	—	—
C_{84}	—	—	4.040	1.273
C_{96}	—	—	4.313	1.293

[a] Average dipole–dipole polarizability.
[b] Reference: calculations carried out with the PAPID program.

volume per atom in the crystalline state is calculated as the weight average for the Sc and C atoms. For all the metallofullerenes, POLAR rather overestimates $<\alpha>$ when compared with PAPID. In particular, when comparing the C_m cages (cf. Table 3) with the corresponding endohedral metallofullerenes, the POLAR $<\alpha>$ increases 154% from C_{60} to $Sc@C_{60}$. This increment is rather overestimated when compared with the PAPID one (32%). The POLAR $<\alpha>$increases ca 18% from C_{82} to $Sc_n@C_{82}$. This increase is under-evaluated with respect to the PAPID one (ca 83%). All

Table 4. Elementary dipole–dipole polarizabilities for the endohedral $Sc_n@C_m$ fullerenes[a]

Endohedral fullerene	v (Å^3)[b]	α (Å^3)[c]	$\alpha_{ref.}$[d]
$Sc@C_{60}$	5.459	3.933	1.193
$Sc@C_{82}$	5.417	4.303	1.026
$Sc_2@C_{82}$	5.531	3.613	1.866
$Sc_3@C_{82}$	5.642	3.976	2.101

[a] α_{bulk} = 1.265 Å^3.
[b] Elementary volume per atom in the crystalline state.
[c] Elementary molecular dipole–dipole polarizability.
[d] Reference: calculations carried out with the PAPID program.

the caged fullerenes computed with POLAR are more polarizable than the bulk. With PAPID, both $Sc_1@C_n$ are less polarizable than the bulk, whereas $Sc_2@C_{82}$ and $Sc_3@C_{82}$ are more polarizable than the bulk.

When comparing Sc_n and C_n, $<\alpha>$ is greater for the three-dimensional (3D) Sc_n clusters than for the two-dimensional C_n clusters. This is due to the 3D character of the metallic bond in Sc_n. The $<\alpha>$ value is greater for the large planar C_n graphite models than for the curved fullerene models owing to the weakening of the π-bonds in the non-planar fullerene structure.

CONCLUSIONS

The polarizability is an important quantity for the identification of clusters with different numbers of atoms and even for the separation of isomers.

The results of the present work clearly indicate that owing to the differences between POLAR and PAPID results, it may become necessary to recalibrate our program POLAR. It appears that the results of good quality *ab initio* calculations might be suitable as primary standards for such a calibration. Work is in progress on the recalibration of POLAR.

The elementary $<\alpha>$ calculated with POLAR increases ca 52% from C_m to endohedral $Sc_n@C_m$. This result is somewhat underestimated compared with the PAPID reference, which gives an increase of ca 70%.

The polarizability trend for the clusters as a function of size is different from what one might have expected. The Sc_n clusters (POLAR and PAPID), C-fullerene and C-graphite (POLAR) are more polarizable than what is inferred from the bulk. The high polarizability of small clusters is attributed to arise from dangling bonds at the surface of the cluster. From this work, recommended elementary polarizability values are 17–22 $Å^3$ (Sc_n), 1.8–1.9 $Å^3$ (small C_n-fullerene), 1.3–1.9 $Å^3$ (small C_n-graphite) and 1.3–1.4 $Å^3$ (large C_n-fullerene and C_n-graphite).

REFERENCES

1. Benichou E, Autoine R, Rayane D, Vezin B, Dalby FW, Dugourd Ph, Broyer M, Ristori C, Chandezon F, Huber BA, Rocco JC, Blundell SA, Guet C. *Phys. Rev. A* 1999; **59**: R1–R4.
2. Maroulis G, Xenides D. *J. Phys. Chem. A* 1999; **103**: 4590–4593.
3. Fuentealba P. *Phys. Rev. A* 1998; **58**: 4232–4234.
4. Fuentealba P, Reyes O. *J. Phys. Chem. A* 1999; **103**: 1376–1380.
5. Jackson K, Pederson M, Wang C-Z, Ho K-M. *Phys. Rev. A* 1999; **59**: 3685–3689.
6. Deng K, Yang J, Chan CT. *Phys. Rev. A* 2000; **61**: 025201–1–4.
7. Deng K, Yang J, Yuan L, Zhu Q. *Phys. Rev. A* 2000; **62**: 045201–1–4.
8. Hohm U, Goebel D, Karamanis P, Maroulis G. *J. Phys. Chem. A* 1998; **102**: 1237–1240.
9. Torrens F, Ruiz-López M, Cativiela C, Garcia JI, Mayoral JA. *Tetrahedron* 1992; **48**: 5209–5218.
10. Torrens F, Sánchez-Marin J, Rivail J-I. *An. Fls. (Madrid)* 1994; **90**: 197–204.
11. Torrens F. *Mol. Simul.* 2000; **24**: 391–410.
12. Silberstein L. *Philos. Mag.* 1917; **33**: 92–128.
13. Silberstein L. *Philos. Mag.* 1917; **33**: 215–222.
14. Silberstein L. *Philos. Mag.* 1917; **33**: 521–533.
15. Applequist J, Carl JR, Fung K-K. *J. Am. Chem. Soc.* 1972; **94**: 2952–2960.
16. Applequist J. *J. Phys. Chem.* 1993; **97**: 6016–6023.
17. Voisin C, Cartier A, Rivail J-L. *J. Phys. Chem.* 1992; **96**: 7966–7971.
18. Voisin C. PhD Thesis, Université de Nancy I, 1991.
19. Birge RR. *J. Chem. Phys.* 1980; **72**: 5312–5319.
20. Fletcher R, Powell MJD. *Comput. J.* 1963; **6**: 163–168.
21. Thole BT. *Chem. Phys.* 1981; **59**: 341–350.
22. Applequist J. *Acc. Chem. Res.* 1977; **10**: 79–85.
23. Torrens F, Sánchez-Marin J, Nebot-Gil I. *J. Mol. Struct. (Theochem)* 1999; **463**: 27–39.
24. Mulliken RS. *J. Chem. Phys.* 1934; **2**: 782–793.
25. Huheey JE. *J. Phys. Chem.* 1965; **69**: 3284–3291.
26. Sanderson RT. *Science* 1951; **114**: 670–672.
27. Mulliken RS, Rieke CA, Orloff D, Orloff H. *J. Chem. Phys.* 1949; **17**: 1248–1267.
28. Joachim C, Treboux G, Tang H. In *Molecular Electronics: Science and Technology*, *AIP Conference Proceedings* vol. 262. American Institute of Physics: New York, 1992; 107–117.
29. Margenau H, Murphy GM (eds). *The Mathematics of Physics and Chemistry*. van Nostrand-Reinhold: New York, 1964.
30. Vogel AI. *J. Chem. Soc.* 1948; 1833–1855.
31. Gresh N, Claverie P, Pullman A. *Int. J. Quantum Chem., Symp.* 1979; **13**: 243–253.
32. Allinger NL. *J. Am. Chem. Soc.* 1977; **99**: 8127–8134.
33. Némethy G, Pottle MS, Scheraga HA. *J. Phys. Chem.* 1983; **87**: 1883–1887.
34. Buckingham AD. *Adv. Chem. Phys.* 1967; **12**: 107–142.
35. Stiehler J, Hinze J. *J. Phys. B* 1995; **28**: 4055–4071.
36. Schäfer R, Schlecht S, Woenckhaus J, Becker JA. *Phys. Rev. Lett.* 1996; **76**: 471–474.
37. Jarrold MF. *Science* 1991; **252**: 1085–1092.
38. De Heer WA. *Rev. Mod. Phys.* 1993; **65**: 611–675.
39. Brack M. *Rev. Mod. Phys.* 1993; **65**: 677–732.
40. Ballard A, Bonin K, Louderback J. *J. Chem. Phys.* 2000; **113**: 5732–5735.
41. Antoine R, Dugourd Ph, Rayane D, Benichou E, Broyer M, Chandezon F, Guet C. *J. Chem. Phys.* 1999; **110**: 9771–9772.
42. Norman P, Luo Y, Jonsson D, Ågren H. *J. Chem. Phys.* 1997; **106**: 8788–8791.
43. Compagnon I, Antoine R, Broyer M, Dugourd P, Lermé J, Rayane D. *Phys. Rev. A* 2001; **64**: 025201–1–4.